3P-31

Proceedings of Symposium on Ultrasonic Electronics, Vol. 31 (2010) pp. 517-518
6-8 December, 2010

Characteristics control of piezoelectric speaker by shape change in piezoelectric bimorph

Huiuk Lee[1†], Jungsoon Kim[2], Moojoon Kim[1] and Kanglyeol Ha[1] ([1]Pukyong National Univ., Korea; [2]Tongmyong Univ., Korea)

1. Introduction

Recently, since electronic devices are becoming more slim in style, the thin-type speaker is demanded to design for the devices. The thin type moving-coil loud speaker has been developed for mobile devices such as mobile phone, GPS, and DMB-TV[1]. However, the speaker needs a massive magnet to induce the driving force for low-range frequencies. To design the thin-type speaker, piezoelectric speakers have been developed using a bimorph or a unimorph actuator. Because of the high quality factor of the piezoelectric vibrator, the frequency range of fidelity of the speaker is limited in narrow bandwidth. In a previous study, we have suggested a method to analyze the performance of bimorph actuator with shape change[2]. It was confirmed that the characteristics of the piezoelectric bimorph actuator varied according to shape. In this study, we suggest the characteristics control method of the speaker by shape change in piezoelectric bimorph. Five different shapes of actuators are fabricated for a wideband characteristic. The speaker, in which the five actuators are arrayed, is designed and its characteristics are investigated.

2. Design of wide-band piezoelectric speaker

The calculation model for the different shape of the piezoelectric bimorph is shown in Fig. 1. The shape of the piezoelectric plates changes as the exponential function changes as indicated in the Fig. 1. As the shape of the piezoelectric bimorph changes, the input admittance is given by[2]

$$Y = j\omega b \frac{d_{32}}{s_{22}^E}\left(\frac{t_p + 2t_m}{2}\right)\sum_{n=1}^{4}\frac{h_n^2}{h_{n+(-1)^{n+1}}}\left(e^{\frac{y}{2}h_{n+(-1)^{n+1}}} - 1\right)C_n + j\omega b\frac{\varepsilon_{33}^{LS}}{t_p}\frac{2}{\alpha}\left(e^{\alpha l} - 1\right) . \qquad (1)$$

Here the each constant C_i is denoted by

$$C_i = \frac{1}{|A|}\begin{bmatrix} \alpha_1\{\varepsilon_{2j}(\varepsilon_{3k}\varepsilon_{4l} - \varepsilon_{3l}\varepsilon_{4k}) - \varepsilon_{2k}(\varepsilon_{3j}\varepsilon_{4l} - \varepsilon_{3l}\varepsilon_{4j}) + \varepsilon_{2l}(\varepsilon_{3j}\varepsilon_{4k} - \varepsilon_{3k}\varepsilon_{4j})\} \\ +\alpha_3\{\varepsilon_{1j}(\varepsilon_{2k}\varepsilon_{4l} - \varepsilon_{2l}\varepsilon_{4k}) - \varepsilon_{1k}(\varepsilon_{2j}\varepsilon_{4l} - \varepsilon_{2l}\varepsilon_{4j}) + \varepsilon_{1l}(\varepsilon_{2j}\varepsilon_{4k} - \varepsilon_{2k}\varepsilon_{4j})\} \\ -\alpha_4\{\varepsilon_{1j}(\varepsilon_{2k}\varepsilon_{3l} - \varepsilon_{2l}\varepsilon_{3k}) - \varepsilon_{1k}(\varepsilon_{2j}\varepsilon_{3l} - \varepsilon_{2l}\varepsilon_{3j}) + \varepsilon_{1l}(\varepsilon_{2j}\varepsilon_{3k} - \varepsilon_{2k}\varepsilon_{3j})\} \end{bmatrix}, \quad (i, j, k, l = 1,2,3,4),$$

where, the factors of the constant are

$\varepsilon_{1n} = 1$, $\varepsilon_{2n} = h_n$, $\varepsilon_{3n} = h_n^2 e^{-h_n l/2}$, $\varepsilon_{3n} = h_n^2 e^{-h_n l/2} h_{n+(-1)^{n+1}}$, n=1~4,

for fixed end at y=0, and

$\varepsilon_{1n} = e^{-h_n l/2}$, $\varepsilon_{2n} = h_n e^{-h_n l/2}$, $\varepsilon_{3n} = h_n^2$, $\varepsilon_{3n} = h_n^2 h_{n+(-1)^{n+1}}$, n=1~4,

for fixed end at y=l, and

$$|A| = \begin{bmatrix} \varepsilon_{11}\{\varepsilon_{22}(\varepsilon_{33}\varepsilon_{44} - \varepsilon_{34}\varepsilon_{43}) - \varepsilon_{23}(\varepsilon_{32}\varepsilon_{44} - \varepsilon_{34}\varepsilon_{42}) + \varepsilon_{24}(\varepsilon_{32}\varepsilon_{43} - \varepsilon_{33}\varepsilon_{42})\} \\ -\varepsilon_{21}\{\varepsilon_{12}(\varepsilon_{33}\varepsilon_{44} - \varepsilon_{34}\varepsilon_{43}) - \varepsilon_{13}(\varepsilon_{32}\varepsilon_{44} - \varepsilon_{34}\varepsilon_{42}) + \varepsilon_{14}(\varepsilon_{32}\varepsilon_{43} - \varepsilon_{33}\varepsilon_{42})\} \\ +\varepsilon_{31}\{\varepsilon_{12}(\varepsilon_{23}\varepsilon_{44} - \varepsilon_{24}\varepsilon_{43}) - \varepsilon_{13}(\varepsilon_{22}\varepsilon_{44} - \varepsilon_{24}\varepsilon_{42}) + \varepsilon_{14}(\varepsilon_{22}\varepsilon_{43} - \varepsilon_{23}\varepsilon_{42})\} \\ -\varepsilon_{41}\{\varepsilon_{12}(\varepsilon_{23}\varepsilon_{34} - \varepsilon_{24}\varepsilon_{33}) - \varepsilon_{13}(\varepsilon_{22}\varepsilon_{34} - \varepsilon_{24}\varepsilon_{32}) + \varepsilon_{14}(\varepsilon_{22}\varepsilon_{33} - \varepsilon_{23}\varepsilon_{32})\} \end{bmatrix}.$$

Here

$h_1 = \alpha + \sqrt{\alpha^2 - 4k_p^2}$, $h_2 = \alpha - \sqrt{\alpha^2 - 4k_p^2}$, $h_3 = \alpha + \sqrt{\alpha^2 + 4k_p^2}$, $h_4 = \alpha - \sqrt{\alpha^2 + 4k_p^2}$,

$\alpha_1 = \alpha^2 N/(k_p^4 K_M)$, $\alpha_3 = 4N/K_M$, $\alpha_4 = 8\alpha N/K_M$,

$\alpha = \frac{1}{l}\ln\left(\frac{a}{b}\right)$, $N = (t_p + 2t_m)\frac{d_{32}}{s_{22}^E}$,

$$K_M = \frac{2}{3}t_m^3 + \frac{2}{s_{22}^E(1 - k_{32}^2)}\left\{\frac{t_p(t_p^2 + 3t_p t_m + 3t_m^2)}{3} - \frac{t_p(t_p + 2t_m)^2 k_{32}^2}{4}\right\}.$$

To investigate the bandwidth of the speaker, the power transfer function is introduced as following equation[3].

$$H_p(\omega) = \frac{4R_g R_m}{\{R_g + R_m\}^2 + \left\{X_m - \frac{1}{\omega C_0}\right\}^2} . \qquad (2)$$

where R_g, R_m, and X_m are internal resistance, motional resistance and reactance, respectively.

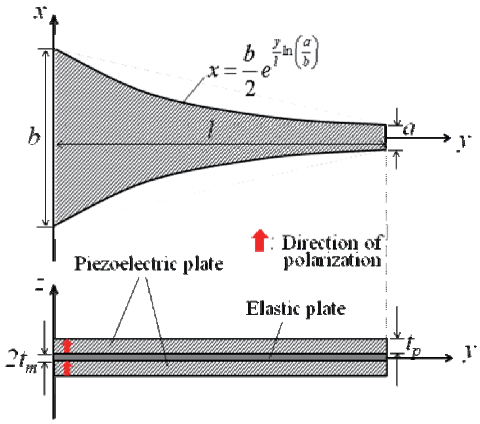

Fig. 1 Calculation model for bimorph actuator

3. Experiment and results

Five piezoelectric bimorph with different shapes were fabricated as shown in Fig. 2. The size of the actuators and the boundary conditions are listed in Table I. To satisfy the fixed-end condition,

---

[1]kimmj@pknu.ac.kr

one ends of them were mounted by epoxy resin. The material constants of the piezoelectric plate used in the bimorph are listed in Table II.

Table I Size and boundary condition of the actuators

Fixed point	y=0			y=l	
b=12.7mm	T_{x1}	T_{x2}	T_{x5}	T_{x3}	T_{x4}
l(mm)	36.59	61.95	38.55	50.10	61.2
a(mm)	12.7	6.3	2.54	4.23	3.2

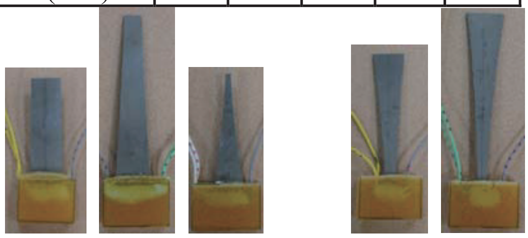

(T_{x1}) (T_{x2}) (T_{x5}) (T_{x3}) (T_{x4})

Fig. 2 Fabricated bimorph actuators

Table II Material constants of the piezoelectric plate

ρ (kg/m^3)	s_{22}^E	k_{32}	ε_{33}^T	d_{32}
7.37×10^3	1.67×10^{-11}	0.39	3.27×10^{-8}	2.81×10^{-10}

Figure 3 shows the input admittance change according to the changes in shape of the actuators. The measured results demonstrate a similar tendency to the theoretical one. In the theoretical calculation, the adhesive layer between the piezoelectric plates was ignored. The admittance slope in the non-resonant frequency range decreases as the b/a ratio is increased because the clamped capacitance is reduced due to the change in electrodes area. Using these actuators, the piezoelectric speaker was fabricated as shown in Fig. 4. The power transfer function of the speaker was measured as shown in Fig. 5. The tendency of the experimental results is similar to the theoretical results. The experimental results are also compared with those of the conventional one. From these results, it was confirmed that the suggested speaker was improved in dynamic frequency range.

4. Conclusion

A wideband piezoelectric speaker is designed with bimorph actuators. The differently tapered five bimorph actuators are fabricated and arrayed for wideband characteristic. The characteristics of the fabricated speaker are measured and compared with theoretical results. The experimental results coincide well with theoretical ones. Using this method, we can expect that a wideband acoustic speaker could be designed.

Acknowledgment

This work was supported by the Korea Research Foundation Grant funded by the Korean Government (MOEHRD, Basic Research Promotion Fund) (KRF-2008-331-D00222).

References

1. H. Takewa, S. Saiki, S. Kano, and A. Inaba: IEEE Trans. Consumer 190 Electronics, **52** (2006) 189.
2. J. Kim, M. Kim, H Lee, and K. Ha: Jpn. J. Appl. Phys. **49** (2010) 07HD08.
3. V. Ristic: *Principles of Acoustic Devices* (John Wiley & Sons, New York, 1983) p. 156.

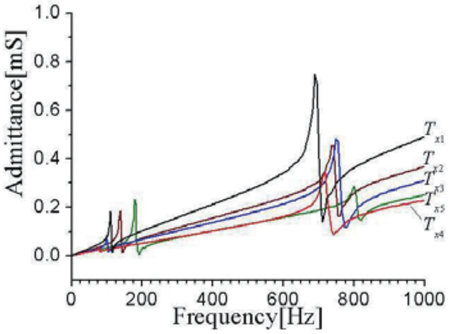

(a) Experiment

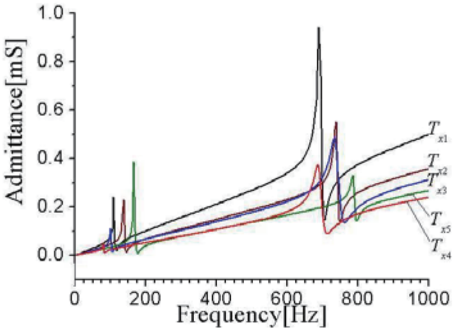

(b) Theory

Fig. 3 Input admittance change with shape

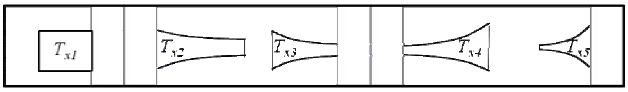

(a)

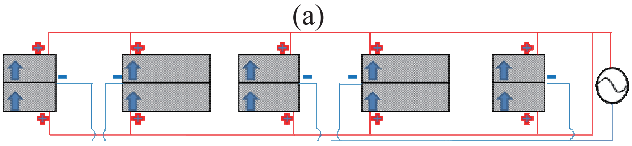

(b)

Fig. 4 Construction of the speaker
(a) Array of the bimorph (b) Driving circuit

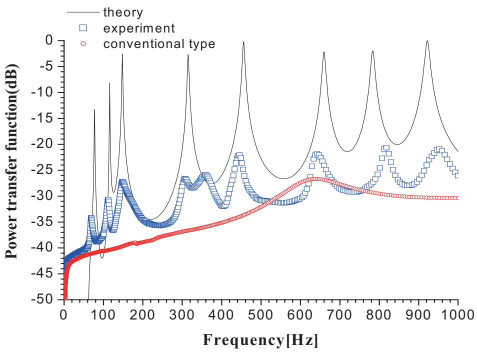

Fig. 5 Power transfer function